**Original Article**
Basic Research

Diabetes Metab J 2023;47:500-513
https://doi.org/10.4093/dmj.2022.0110
pISSN 2233-6079 · eISSN 2233-6087

dmj
DIABETES & METABOLISM JOURNAL



# Beneficial Effects of a Curcumin Derivative and Transforming Growth Factor-β Receptor I Inhibitor Combination on Nonalcoholic Steatohepatitis

Kyung Bong Ha[1,2,*], Eun Soo Lee[1,2], Na Won Park[1,2], Su Ho Jo[1,2], Soyeon Shim[3], Dae-Kee Kim[3], Chan Mug Ahn[4], Choon Hee Chung[1,2]

[1]Department of Internal Medicine, Yonsei University Wonju College of Medicine, Wonju,
[2]Research Institute of Metabolism and Inflammation, Yonsei University Wonju College of Medicine, Wonju,
[3]Department of Pharmacy, College of Pharmacy, Ewha Womans University, Seoul,
[4]Department of Basic Science, Yonsei University Wonju College of Medicine, Wonju, Korea

**Background:** Curcumin 2005-8 (Cur5-8), a derivative of curcumin, improves fatty liver disease via AMP-activated protein kinase activation and autophagy regulation. EW-7197 (vactosertib) is a small molecule inhibitor of transforming growth factor β (TGF-β) receptor I and may scavenge reactive oxygen species and ameliorate fibrosis through the SMAD2/3 canonical pathway. This study aimed to determine whether co-administering these two drugs having different mechanisms is beneficial.
**Methods:** Hepatocellular fibrosis was induced in mouse hepatocytes (alpha mouse liver 12 [AML12]) and human hepatic stellate cells (LX-2) using TGF-β (2 ng/mL). The cells were then treated with Cur5-8 (1 μM), EW-7197 (0.5 μM), or both. In animal experiments were also conducted during which, methionine-choline deficient diet, Cur5-8 (100 mg/kg), and EW-7197 (20 mg/kg) were administered orally to 8-week-old C57BL/6J mice for 6 weeks.
**Results:** TGF-β-induced cell morphological changes were improved by EW-7197, and lipid accumulation was restored on the administration of EW-7197 in combination with Cur5-8. In a nonalcoholic steatohepatitis (NASH)-induced mouse model, 6 weeks of EW-7197 and Cur5-8 co-administration alleviated liver fibrosis and improved the nonalcoholic fatty liver disease (NAFLD) activity score.
**Conclusion:** Co-administering Cur5-8 and EW-7197 to NASH-induced mice and fibrotic hepatocytes reduced liver fibrosis and steatohepatitis while maintaining the advantages of both drugs. This is the first study to show the effect of the drug combination against NASH and NAFLD. Similar effects in other animal models will confirm its potential as a new therapeutic agent.

**Keywords:** ALK5 inhibitor; Curcumin; Fibrosis; Non-alcoholic fatty liver disease; Transforming growth factor beta

## INTRODUCTION

Nonalcoholic fatty liver disease (NAFLD), whose incidence is on the rise, is the most common cause of chronic liver disease [1,2]. NAFLD includes liver steatosis ranging from simple steatosis to nonalcoholic steatohepatitis (NASH), liver fibrosis, cirrhosis, and alcohol-independent steatosis [3]. Metabolic overload that stresses hepatocytes causes cellular damage, inflammation, and fibrosis, affecting the liver, adipose tissue, endocrine pancreas, immune system, and intestines. Attempts have been made to develop NASH treatments [4].

Excessive fat accumulation in the liver initially reduces hepatic wound healing response and chronically accumulates extracellular matrix (ECM), causing fibrosis [5,6]. Collagen I (ColI) and α-smooth muscle actin (α-SMA) accumulate in wounded liver tissues during fibrosis. Pro-fibrotic cytokines

Corresponding author: Choon Hee Chung https://orcid.org/0000-0003-1144-7206
Department of Internal Medicine, Yonsei University Wonju College of Medicine,
20 Ilsan-ro, Wonju 26426, Korea
E-mail: cchung@yonsei.ac.kr

*Current affiliation: Division of Cardiovascular Disease Research, Department of Chronic Disease Convergence Research, Korea National Institute of Health, Cheongju, Korea

Received: Apr. 1, 2022; Accepted: Jul. 19, 2022

and their intracellular signaling pathways, particularly transforming growth factor β (TGF-β)-mediated SMAD signaling, are also characteristic of liver fibrosis [7,8]. TGF-β is a major factor in tissue fibrosis, acting through SMAD2/3 signaling, promoting ECM production, reactive oxygen species (ROS) generation, and myofibroblast activation [9]. TGF-β binds to type II receptor (TβRII) serine/threonine kinase and recruits plasma membrane type I receptor (TβRI) to form a receptor dimer. Signal transduction is then activated through SMAD2/3 phosphorylation [10]. Phosphorylated SMAD2/3 forms a heterogenic complex with SMAD4 and is translocated to the nucleus where target genes are transcribed [11,12]. TGF-β also activates non-canonical signaling pathways, including extracellular signal-regulated kinase (ERK), JNK, and p38 mitogen-activated protein kinase (MAPK) [13].

Curcumin (Cur) is the primary bioactive substance in turmeric and alleviates metabolic syndrome, pain, and kidney damage through its anti-inflammatory and antioxidant effects [14,15]. However, it has disadvantages, including low water solubility, low absorption in the intestines, rapid metabolic processing, and systemic elimination [16]. Curcumin 2005-8 (Cur5-8), a Cur derivative, significantly inhibits high-fat diet-induced NAFLD by reducing fat synthesis via AMP-activated protein kinase (AMPK) activation and autophagy regulation [17].

TGF-β signaling is a potential target for preventing and treating fibrotic diseases, and directly inhibiting the TGF-β type I receptor, activin receptor-like kinase 5 (ALK5) prevents TGF-β-induced pro-fibrosis. TGF-β RI inhibitors compete with the ATP-binding site of ALK5 to block the highly specific catalytic activity of ALK5 [18]. EW-7197 (vactosertib), a small molecule inhibitor of the TGF-β type I receptor, is an oral drug that improves kidney, lung, and liver fibrosis. EW-7197 regulates ROS by reducing NADPH oxidase, nuclear factor erythroid 2-related factor 2 (Nrf2), and heme oxygenase-1 (HO-1) levels and prevents fibrosis by inhibiting TGF-β inhibition [18-20].

Cur5-8 is a Cur analog that improves body weight, blood glucose, and fatty liver [17]. This study used a 12-week high-fat diet-induced NAFLD animal model that shows fatty liver or mild inflammatory responses but does not progress to steatohepatitis or fibrosis [21].

We previously showed that EW-7197 can ameliorate diabetic nephropathy in the *db/db* mouse model. Analysis of kidneys following 12 weeks of oral administration of EW-7197 (20 mg/kg) demonstrated improved renal function, and renal fibrosis [21]. EW-7197 improved fibrosis but not body weight and blood glucose. Additionally, EW-7197 increased the number of lipid droplets in the liver.

This study analyzed the effect of Cur5-8 on fatty liver and fibrosis in mice fed a methionine-choline-deficient diet (MCD) diet. We hypothesized that EW-7197 improves fibrosis and that Cur5-8 improve NAFLD/NASH by reducing lipid droplets in the liver. This study aimed to determine whether EW-7197 and Cur5-8 act synergistically to reduce hepatotoxicity and whether they have potential as new therapeutic agents for NASH.

## METHODS

### Reagents

Cur was purchased from Santa Cruz Biotechnology (Dallas, TX, USA). And then chemically modified to form Cur5-8 at Department of Basic Science, Yonsei University, Wonju College of Medicine [16]. Cur5-8 was synthesized at Uchem Inc. (Shanghai, China). *N*-[[4-([1,2,4]-triazolo[1,5-a]pyridin-6-yl)-5-(6-methylpyridin-2-yl)-1*H*-imidazol-2-yl]methyl]-2-fluoroaniline (EW-7197) was kindly donated by Dr. D.K.K. (Ewha Womans University, Seoul, Korea).

### Animals

Mouse experiments were approved by the Institutional Animal Care and Use Committee of Yonsei University, Wonju College of Medicine (YWC-200907-1). Eight-week-old C57BL/6J male mice weighing 20 to 25 g were purchased from Daehan Bio Link Co. (Eumseong, Korea) and acclimatized to 24°C±2°C, and a 12-hour light/dark cycle for 1 week. They were fed a normal diet and provided with water *ad libitum*. Mice were randomly divided into five groups based on the feed or drug administered ($n=10$): normal diet (Con), MCD, MCD diet with Cur5-8 (MCD+Cur5-8), MCD diet with orally-administered EW-7197 (MCD+EW), and MCD diet with Cur5-8 and orally-administered EW-7197 (MCD+EW+Cur5-8). EW-7197 was dissolved in concentrated gastric fluid (900 mL dd$H_2O$, 7 mL 37% HCl, 2.0 g NaCl, and 3.2 g pepsin) and diluted with phosphate-buffered saline in a 1:10 ratio. Diluted gastric juice was administered as a vehicle to mice in the Con and MCD groups. EW-7197 (40 mg/kg) was administered orally once every 2 days for 6 weeks.

### Metabolic parameters

Blood glucose, triglyceride (TG), total cholesterol (TC), and

liver enzyme levels (alanine transaminase [ALT] and aspartate transaminase [AST]) were measured using a reagent for measurement in serum at the end of the experiment (Asan Pharm., Hwaseong, Korea), and the degree of change in absorbance was measured using a SpectraMax (Molecular devices, Los Angeles, CA, USA). Hepatic gamma-glutamyl transferase (γ-GT, Sigma Aldrich, St. Louis, MO, USA) and hydroxyproline (Cell Biolabs Inc., San Diego, CA, USA) were measured using kits.

**Cell culture**

Alpha mouse liver 12 (AML12) mouse hepatocytes were cultured in Dulbecco's Modified Eagle's Medium (DMEM)/F-12 media (Corning Inc., Corning, NY, USA) containing 5 mL insulin-transferrin-selenium (Gibco, Life Technologies Corporation, Grand Island, NY, USA), 40 ng/mL dexamethasone, 1% penicillin-streptomycin, and 10% fetal bovine serum (FBS, Gibco). human hepatic stellate cells (LX-2) human hepatic stellate cells (HSCs) were cultured in high glucose media (4,500 mg/L D-glucose, L-glutamine, 110 mg/L sodium pyruvate, sodium bicarbonate) containing 1% penicillin-streptomycin and 10% FBS. Hepatocellular fibrosis was induced in cells using 2 ng/mL of TGF-β and treated with EW-7197 (500 nM), Cur (1 μM), and Cur5-8 (1 μM) for 24 hours.

**Immunofluorescence assay**

Cultured AML12 cells were fixed in BD Cytofix (BD Bioscience, Franklin Lakes, NJ, USA) for 15 minutes at 24°C±2°C, and then treated with 0.1% Triton X-100 (Sigma-Aldrich) for 10 minutes. The primary antibody 8-OHdG (Santa Cruz Technology) was diluted at 1:200 with 3% bovine serum albumin (BSA) and incubated overnight at 4°C. The secondary antibody, anti-mouse immunoglobulin G (Alexa Fluor 488, Cell Signaling, Danvers, MA, USA) was diluted at 1:500 with 3% BSA and incubated with the cells for 1 hour. 4′,6-Diamidino-2-phenylindole (DAPI) stock solution (Abcam, Cambridge, England) was incubated with the cells 1 mL/0.5 μL for 15 minutes. After that, the cells were mounted in Immu-Mount (Thermo Fisher Scientific, Waltham, MA, USA), and fluorescence images were taken using a laser scanning confocal microscope (Carl Zeiss Microscopy GmbH, Gottingen, Germany).

**Histological examination**

Tissues were subsequently divided into 8-μm sections and stained with hematoxylin and eosin (H&E) to analyze pathological changes in lipid droplets. Sirius red and Masson's trichrome staining were used to check for fibrosis. H&E-stained sections were visualized using an optical microscope equipped with a charge-coupled device camera (Pulnix, Orleans Drive Sunnyvale, CA, USA). Sections from three hepatic lobes from each animal were analyzed and three random pictures were taken for each section. Analyzed sections were scored based on the following criteria: steatosis scores ranging from 0 to 3 depending on the percentage of lipid droplets in the liver; 0 to 2 depending on the number of hepatocytes in which ballooning occurred; and 0 to 3 depending on the degree of lobular inflammation. The scores were summed up to give a final NASH score.

**Western blotting**

Antibodies against fibronectin (SC-6952), α-SMA (SC-32251), ColI (SC-293182), sterol regulatory element-binding protein 1c (srebp1c) (SC-13551), adipose differentiation-related protein (ADRP) (SC-377429), rho-associated coiled-coil kinase (ROCK) (SC-365628), Nrf2 (SC-722), HO-1 (SC-136960), activating transcription factor 6α (ATF6α) (SC-22799), and β-actin (SC-47778) were obtained from Santa Cruz Technologies. Antibodies against p-SMAD2 (#3108), p-SMAD3 (#9520), phosphor-AMPK (p-AMPK) (#2531), AMPK (#2532), and Kelch-like ECH-associated protein 1 (Keap1) (#4678) were obtained from Cell Signaling Technologies. Proteins were detected using a Western blot assay. Liver tissue homogenized in RIPA buffer (Elpis Biotech, Daejeon, Korea) was centrifuged at 13,000 g for 20 minutes. Supernatant was mixed with sample buffer. Sample was separated by sodium dodecyl sulfate-polyacrylamide gel electrophoresis (8% to 12%). Resolved protein bands were transferred onto polyvinylidene difluoride membranes, and the membranes were incubated with primary and secondary antibodies (diluted 1:1,000 with 5% BSA). Protein bands were visualized using an enhanced chemiluminescence system (Amersham Biosciences, Amersham, UK), and band intensities were measured using ImageJ software version 1.50i (National Institutes of Health, Bethesda, MD, USA).

**Statistical analysis**

Data were analyzed using SPSS software version 20.0 (IBM Co., Armonk, NY, USA). All data are presented as mean± standard error of the mean. One-way analysis of variance (ANOVA) and Tukey's test were used for multiple comparisons. Statistical significance was set at $P<0.05$.

## RESULTS

### Cur5-8 reduces lipid accumulation in hepatocytes

Cell morphology and BODIPY staining were observed under a microscope following 24 hours of oleic acid (OA) treatment. In AML12 cells, OA was combined with Cur, Cur5-8, and EW-7197. Lipids accumulated in the OA-treated group. Cur treatment reduced lipid synthesis slightly, while Cur5-8 reduced lipid synthesis significantly. However, the EW-7197 treatment group showed an increase in cellular lipid accumulation compared with the OA group (Fig. 1A-C). Western blot data also showed that ADRP, the lipogenesis-related protein Srebp1c,

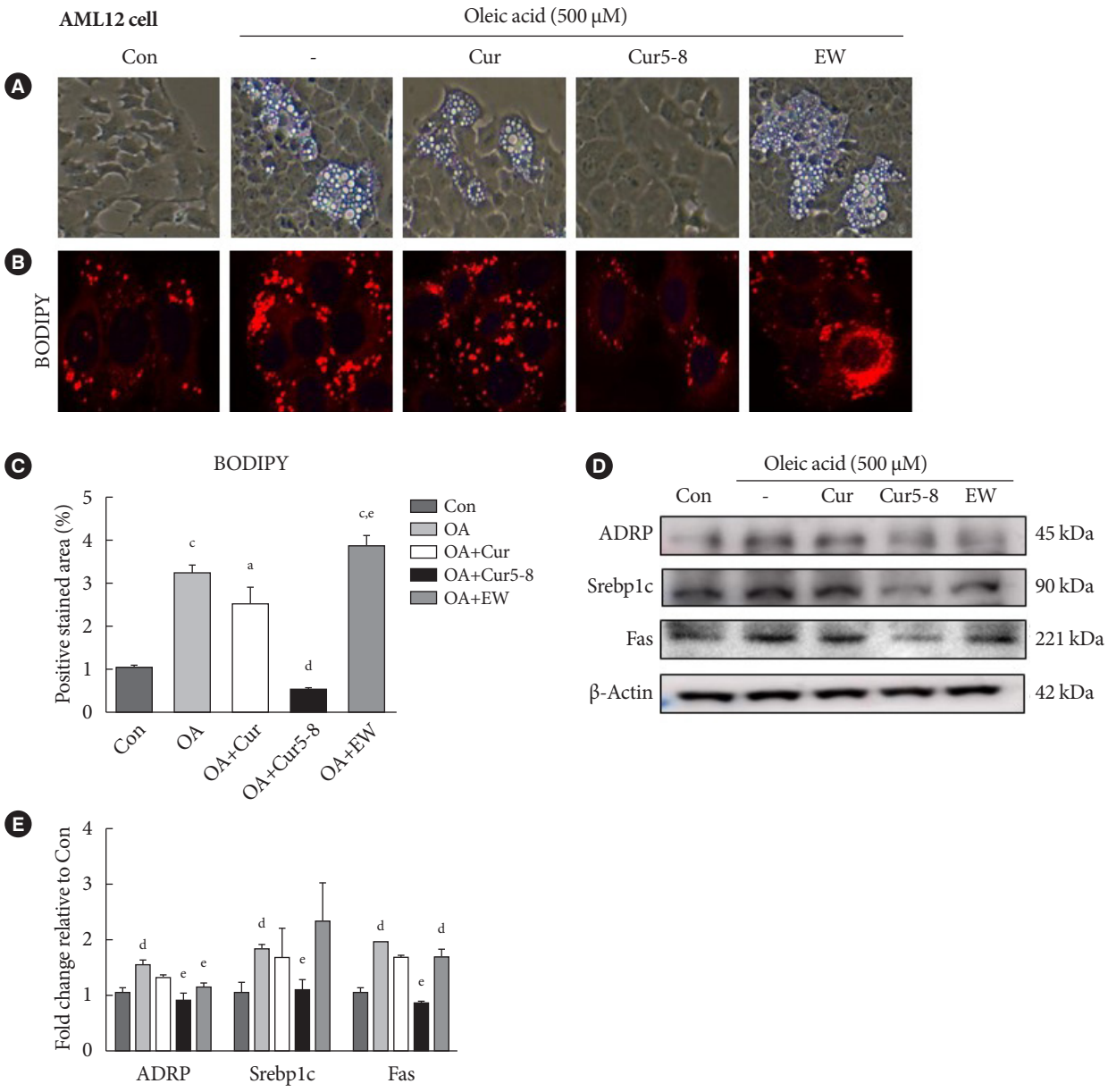


**Fig. 1.** Curcumin 2005-8 (Cur5-8) reduces lipid accumulation in hepatocytes. (A, B, C) Cell morphology and BODIPY staining were observed under a microscope following 24 hours of oleic acid (OA) treatment. In alpha mouse liver 12 (AML12) cells, OA was combined with Cur, Cur5-8, and EW-7197. (D, E) Levels of adipose differentiation-related protein (ADRP), sterol regulatory element-binding protein 1c (Srebp1c), and fatty acid synthase (Fas) were measured using a Western blotting assay. [a]$P<0.001$ vs. control (Con), [b]$P<0.001$ vs. oleic acid, [c]$P<0.001$ vs. oleic acid+Cur5-8, [d]$P<0.05$ vs. Con, [e]$P<0.05$ vs. oleic acid.

and fatty acid synthase (FAS) expression levels were significantly increased following OA treatment, although Cur5-8 treatment resulted in a greater decrease in their expression than Cur treatment. In contrast, EW-7197 treatment increased the levels of these proteins compared with OA treatment (Fig. 1D and E). Cur5-8 decreased lipogenesis-related protein and increased β-oxidation compared to Cur (Supplementary Fig. 1). These results indicate that Cur5-8 has a greater beneficial effect on decreasing lipid synthesis than Cur. However, EW-7197 increases lipid accumulation following OA treatment.

**EW-7197 relieves hepatocellular fibrosis but has side effects**

Treatment of LX-2 cells with TGF-β (2 ng/mL) and EW-7197 significantly reduced TGF-β-induced expression of the fibrosis markers α-SMA and Col I, as well as p-SMAD2/3, compared with TGF-β treatment alone (Fig. 2A and B). Similar results were obtained from AML12 cells (Fig. 2C and D), wherein EW-7197 and TGF-β (TGF-β+EW) treatment significantly reduced α-SMA, Col I, and p-SMAD2/3 expression compared with TGF-β treatment alone. EW-7197 exhibited anti-fibrotic

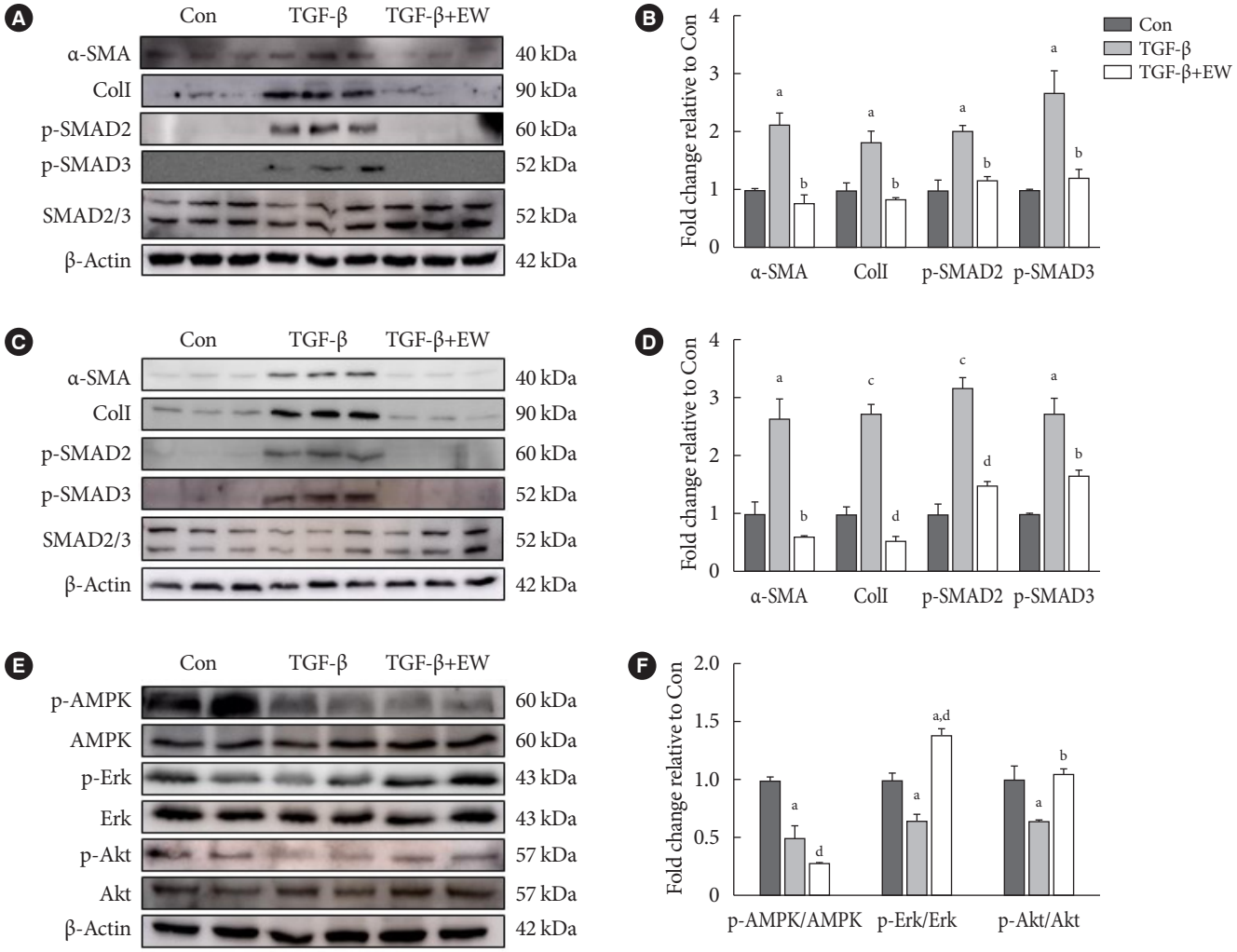


**Fig. 2.** EW-7197 relieves hepatocellular fibrosis but has side effects. Hepatocellular fibrosis was induced by treating human hepatic stellate cell (LX-2) cells with transforming growth factor β (TGF-β; 2 ng/mL). (A, B) The ability of EW-7197 to restore the original state was tested by expressing fibrosis markers such as p-SMAD2/3, α-smooth muscle actin (α-SMA), and ColI. (C, D) Alpha mouse liver 12 (AML12) cells were treated with EW-7197 combined with TGF-β. (E, F) AMP-activated protein kinase (AMPK), extracellular signal-regulated kinase (Erk), and Akt activities were measured to determine the effect of EW-7197 treatment on the TGF-β non-canonical pathway. [a]$P<0.05$ vs. control (Con), [b]$P<0.05$ vs. TGF-β, [c]$P<0.001$ vs. Con, [d]$P<0.001$ vs. TGF-β.

effects but increased the number of lipid droplets, possibly via the non-canonical pathways, AMPK, Erk, and Akt (Fig. 2E and F). Con, Erk, and Akt activities were lower in the TGF-β treatment group but were partially restored in the TGF-β+EW treatment group. However, AMPK activity was lower in the TGF-β treatment group than in the Con group and did not increase in the TGF-β+EW treatment group. Thus, EW-7197 improves fibrosis by inhibiting the TGF-β canonical pathway but does not activate the AMPK pathway.

**Cur5-8 and EW-7197 combination improves TGF-β-induced hepatocellular fibrosis and lipid accumulation**

TGF-β-induced hepatocellular fibrosis is accompanied by changes in cell morphology. Treatment with TGF-β and EW-7197 resulted in significant recovery in cellular morphology compared with TGF-β treatment alone. However, this drug combination increased lipid accumulation (Fig. 3A). Treatment with Cur or Cur5-8 combined with TGF-β did not alter TGF-β-induced fibrosis. However, treating AML12 cells with a

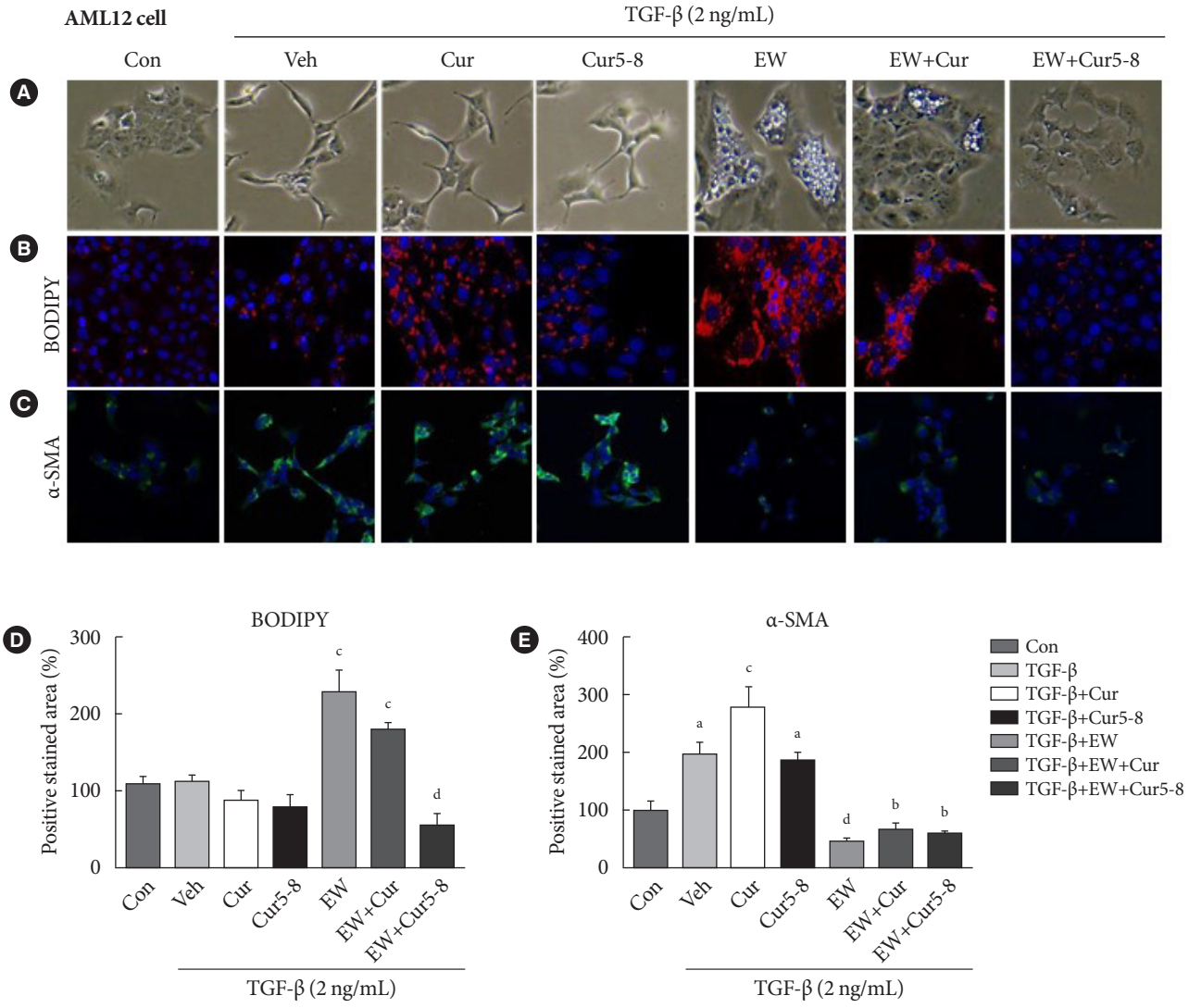


**Fig. 3.** Curcumin 2005-8 (Cur5-8) and EW-7197 improves transforming growth factor β (TGF-β)-induced hepatocellular fibrosis and lipid accumulation. Hepatocellular fibrosis was induced in alpha mouse liver 12 (AML12) cells using TGF-β. The cells were then treated with Cur, Cur5-8, and EW-7197, individually or in combination (EW+Cur or EW+Cur5-8). (A) Changes in cell morphology were then visualized. (B, D) Lipid accumulation in hepatocytes was visualized using BODIPY staining. (C, E) The degree of fibrosis and lipid droplet accumulation was determined using α-smooth muscle actin (α-SMA) staining and by measuring the BODIPY-positive stained area. Veh, vehicle. [a]$P<0.05$ vs. control (Con), [b]$P<0.05$ vs. TGF-β, [c]$P<0.001$ vs. Con, [d]$P<0.001$ vs. TGF-β.

combination of Cur5-8, EW-7197, and TGF-β significantly reduced cellular morphological changes without increasing lipids compared with TGF-β and Cur combination treatment (Fig. 3B and D). Unlike EW-7197, Cur and Cur5-8 had no inhibitory effect on α-SMA; however, combining them with EW-7197 significantly reduced TGF-β-induced α-SMA expression (Fig. 3C and E). Similar results were obtained using LX-2 cells. Morphological changes were not observed in LX-2 cells following TGF-β treatment, although α-SMA expression increased. Additionally, α-SMA expression decreased in the EW-7197 treatment group (Supplementary Fig. 2A-C). EW-7197 treatment increased the number of lipid droplets, and co-administering it with Cur5-8 reduced hepatocellular fibrosis and reduced the number of lipid droplets (Supplementary Fig. 2D and E). These data indicate that EW-7197 and Cur5-8 co-treatment is more effective at inhibiting fibrosis and lipid synthesis than single-drug treatment.

**Combining Cur5-8 and EW-7197 reduces hepatic fibrosis**

Expression of the epithelial-mesenchymal transition (EMT)-related proteins, α-SMA and ColI, in LX-2 cells was increased following TGF-β-treatment. In the canonical TGF-β signaling pathway, p-SMAD2/3 was also increased by TGF-β (Fig. 4A and B). These increases were inhibited by EW-7197 and significantly decreased in the EW+Cur5-8 treatment group compared with that in the TGF-β treatment group. Co-administration of Cur 5-8 and EW-7197 also reduced the activation of fibrosis markers by TGF-β in AML12 cells (Fig. 4C and D). Cur and Cur5-8 had no significant effect on fibrotic markers, whereas EW-7197 reduced the expression of fibrotic markers.

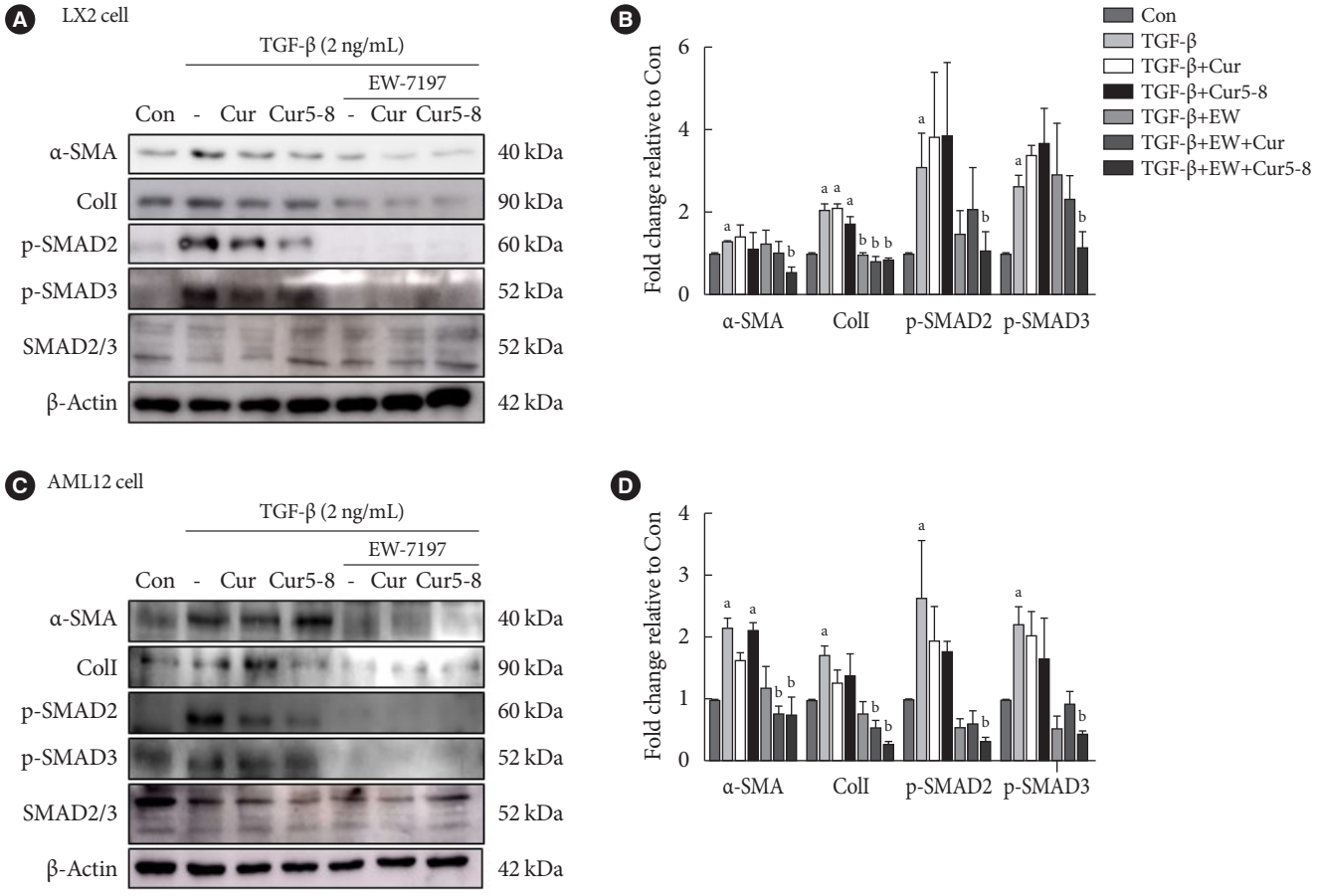


**Fig. 4.** Combinning curcumin 2005-8 (Cur5-8) and EW-7197 reduces hepatic fibrosis. To determine the effect of co-administering different combinations, we added Cur, Cur5-8, and EW-7197 separately to human hepatic stellate cell (LX-2) cells treated with transforming growth factor β (TGF-β). We also added EW-7197+Cur and EW-7197+Cur5-8 combinations. Levels of p-SMAD 2/3 proteins, members of the canonical pathway of TGF-β, α-smooth muscle actin (α-SMA), and ColI proteins, which are markers of fibrosis, were measured in (A, B) LX-2 cells and (C, D) AML12 cells. [a]$P<0.05$ vs. control (Con), [b]$P<0.05$ vs. TGF-β.

These results indicate that co-administering EW-7197 and Cur5-8 effectively inhibits fibrosis in hepatocytes.

**Combining Cur5-8 and EW-7197 improves hepatic function**

Physiological levels of TG, cholesterol, AST, and ALT in serum were measured following Cur5-8 and EW-7197 administration, individually or in combination, to mice in the liver fibrosis-induced MCD group. Body weight and TC and TG levels were lower in mice in the MCD group than in the Con group, while AST and ALT levels were higher. Cur5-8 and EW-7197, on their own, did not affect these levels (Supplementary Table 1, Supplementary Fig. 3A and B). The MCD diet suppresses the production of very-low-density lipoproteins and promotes inflammation and lipogenesis in the liver. It is thus characterized by a decrease in TG and cholesterol levels in the serum [22]. Analysis of hydroxyproline, a fibrosis factor, showed that TG and cholesterol levels in the combined administration group were significantly lower than in the MCD group, and analysis of γ-GT showed that the combined administration group had significantly lower TG and cholesterol levels than the MCD group (Supplementary Fig. 3C and D). EW-7197 effectively inhibited liver fibrosis, and ALT levels decreased in the Cur5-8, EW-7197, and Cur+EW-7197 groups compared with that in the MCD group. These results show that co-administering the two drugs is beneficial as it combines the fibrotic effect of EW-7197 with the antioxidant potential of Cur5-8.

**Cur5-8 and EW-7197 co-administration improves hepatic lipid accumulation**

At the end of the experiment, mouse livers were weighed and hepatic fat accumulation was evaluated using H&E staining. NAFLD activity scores (NAS) were computed, and the degree of steatosis was determined using H&E staining (Fig. 5A-C). NASH was induced in the MCD group, and NAS was significantly lower in the MCD+EW+Cur group than in the Con group. Hepatic fibrosis was inhibited by EW-7197, but mice in the MCD+EW group had higher NAS than those in the Con group due to a higher number of lipid droplets in the liver. Co-administering Cur5-8 and EW-7197 improved fibrosis and reduced the lipid content, and the NAS of the MCD+EW+Cur5-8 group was significantly lower than that of the MCD group. Hepatic lipogenesis was investigated by measuring Rock1 and Srebp1c protein levels and AMPK activity (Fig. 5D). Rock1 and Srebp1c levels were higher, while AMPK activity was lower in the MCD group than in the Con group. Furthermore, Rock1 and Srebp1c levels were significantly lower, while AMPK activity was higher in the MCD+EW+Cur5-8 group than in the MCD group. Analysis of endoplasmic reticulum (ER) stress showed that ATF-6α levels were significantly higher in the MCD group and lower in the MCD+EW+Cur5-8 group than in the Con group. Levels of ROS scavenger markers, Kelch-like ECH-associated protein 1 (Keap1), Nrf2, and HO-1 decreased in the MCD group and increased in the MCD+EW+Cur5-8 group compared with that in the Con group (Fig. 5E and F). EW-7197 and Cur5-8 co-administration inhibited lipogenesis by activating liver metabolism, reducing ROS, and regulating ER stress.

**Cur5-8 and EW ameliorate liver fibrosis**

Sirius red and trichrome staining were used to visualize hepatic fibrosis (Fig. 6A and B). The positive stained area showed that fibrosis was induced in the MCD group and did not recover in the MCD+Cur5-8 group (Fig. 6C). The positively-stained area identified using both staining methods showed that fibrosis and fat accumulation were significantly higher in the MCD group than in the Con group. ColI, α-SMA, fibronectin, and p-SMAD2/3 levels were higher in the MCD group than in the Con group (Fig. 6D and E). Expression of fibrotic markers was significantly lower in the MCD+EW+Cur5-8 group than in the Con group. Cur5-8 did not affect liver fibrosis, whereas EW-7197 improved liver fibrosis but resulted in lipid accumulation in hepatocytes. Combining Cur5-8 and EW-7197 inhibited hepatic fibrosis and reduced the accumulation of hepatic lipid droplets.

## DISCUSSION

To investigate the effects of EW-7197 and Cur5-8, a Cur derivative, on lipogenesis, 500 μM of OA was added to AML12 hepatocytes to induce lipogenesis. Cell morphology and BODIPY staining identified lipid droplets within hepatocytes. Cur5-8 inhibited the increase in lipid droplets observed after adding OA. To determine whether OA induced lipogenesis in AML12 hepatocytes and whether Cur, Cur5-8, and EW-7197 inhibited lipogenesis, lipid droplets were identified through cell morphology and BODIPY staining. The increase in lipid droplets following the addition of OA was inhibited by Cur5-8. ADRP and Srebp1c expression were significantly lower in the Cur5-

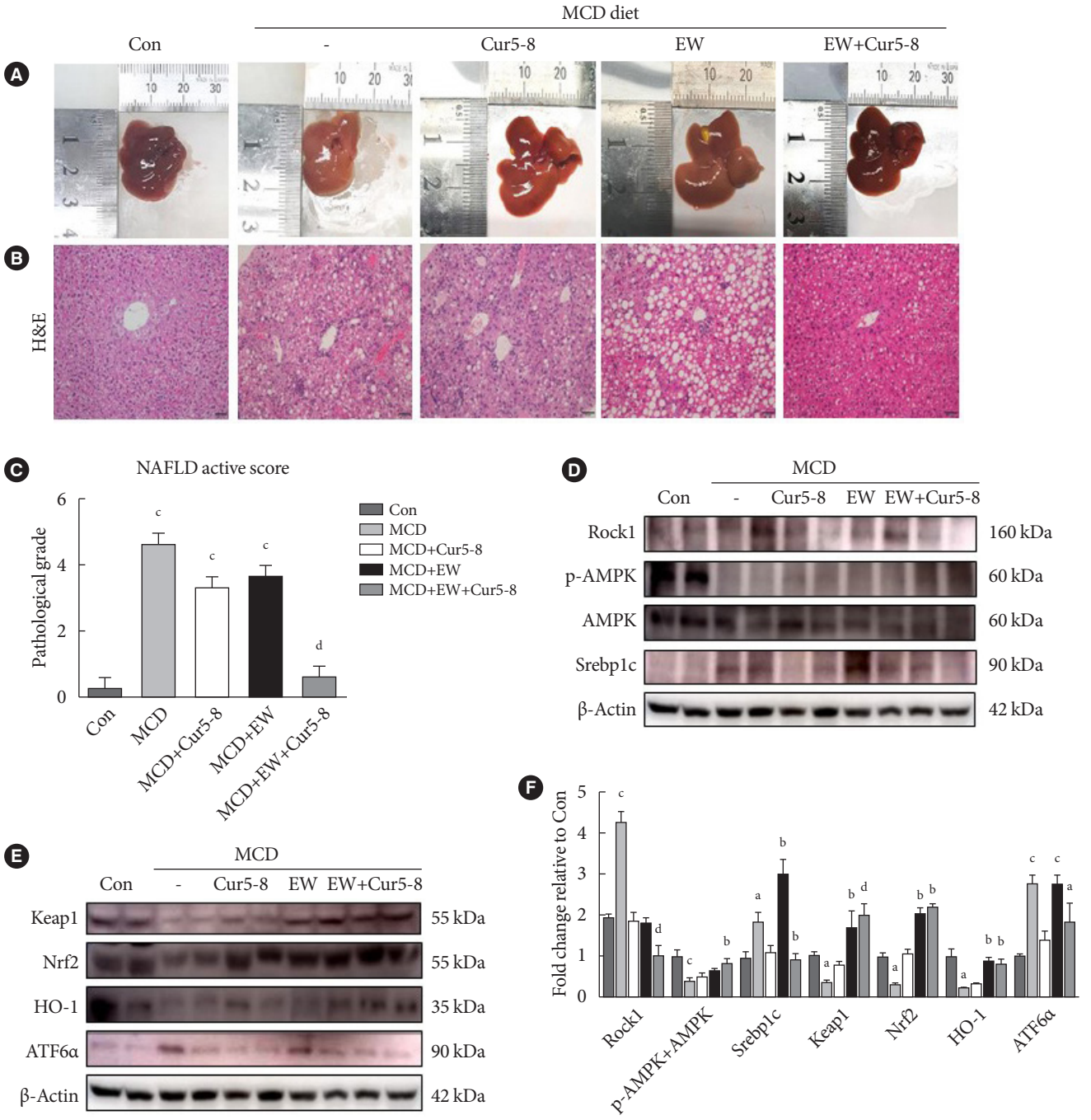


**Fig. 5.** Curcumin 2005-8 (Cur5-8) and EW-7197 co-administration improves hepatic lipid accumulation. (A, B) Accumulation of lipid droplets and variations in liver sizes were measured using H&E staining and liver imaging, respectively. (C) Nonalcoholic fatty liver disease (NAFLD) activity was scored by quantifying the degree of steatosis, hepatocyte ballooning, and lobular inflammation based on the results of H&E staining. (D, E, F) The NAFLD activity score is assigned as described in the Methods section. Metabolism-related proteins were determined by measuring rho-associated coiled-coil kinase 1 (Rock1) and sterol regulatory element-binding protein 1c (Srebp1c) levels, AMP-activated protein kinase (AMPK) activity, and reactive oxygen species (ROS) scavenging effect. Endoplasmic reticulum stress regulation was determined by measuring Kelch-like ECH-associated protein 1 (Keap1), nuclear factor erythroid 2-related factor 2 (Nrf2), heme oxygenase-1 (HO-1), and activating transcription factor 6α (ATF6α) levels. [a]$P<0.05$ vs. control (Con), [b]$P<0.05$ vs. methionine-choline-deficient diet (MCD), [c]$P<0.001$ vs. Con, [d]$P<0.001$ vs. MCD.

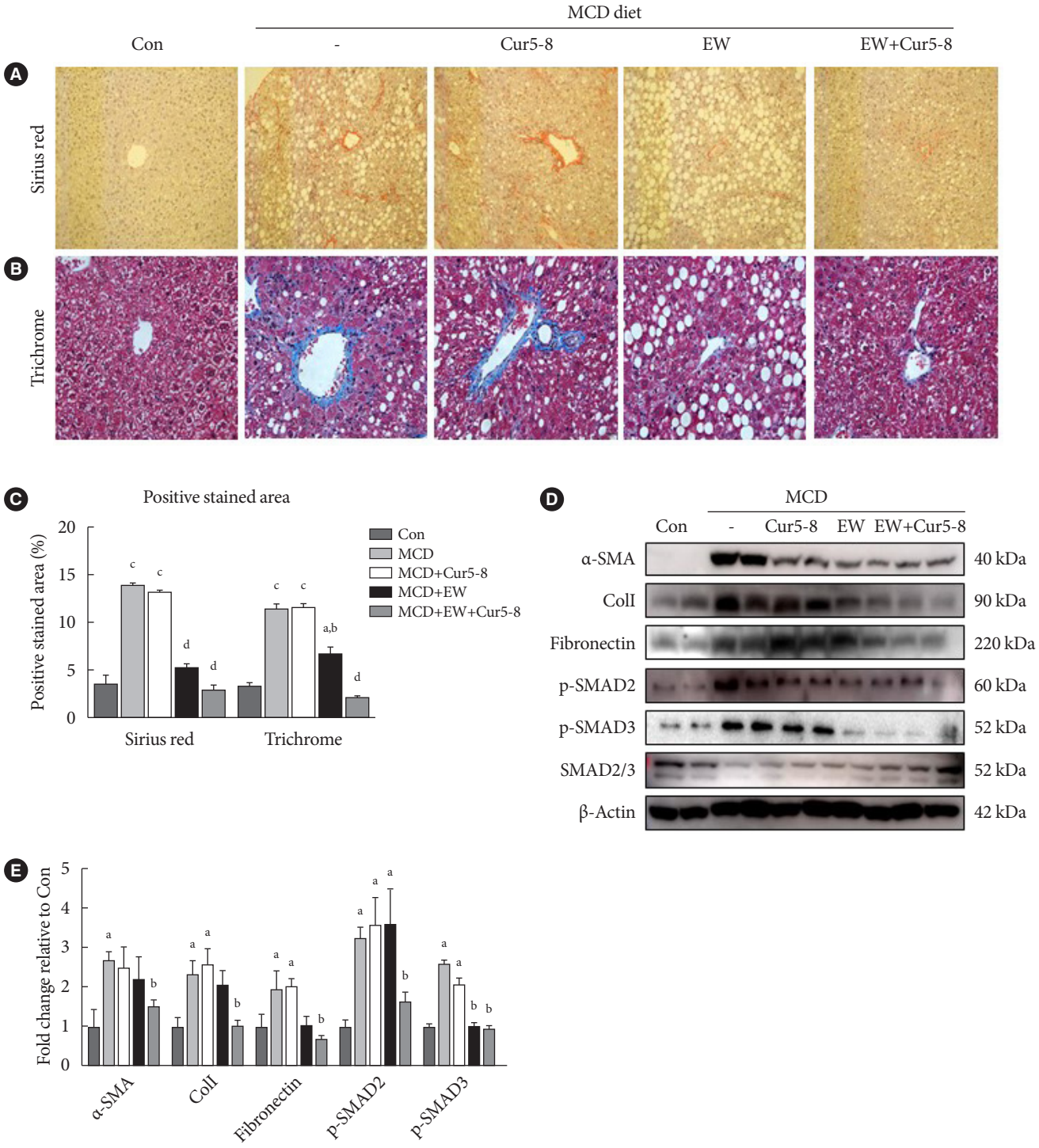


**Fig. 6.** Curcumin 2005-8 (Cur5-8) and EW ameliorate liver fibrosis. (A, B, C) Liver fibrosis was measured using Sirius red and trichrome staining. The degree of liver fibrosis in the experimental groups was compared by quantifying the positively-stained area. (D, E) Levels of extracellular matrix-related α-smooth muscle actin (α-SMA), collagen I (ColI), fibronectin, and transforming growth factor β (TGF-β) canonical pathway-related p-SMAD2/3 were measured. [a]$P<0.05$ vs. control (Con), [b]$P<0.05$ vs. methionine-choline-deficient diet (MCD), [c]$P<0.001$ vs. Con, [d]$P<0.001$ vs. MCD.

8-treated group than in the OA-treated group. EW-7197 and OA co-administration increased lipid accumulation and Srebp1c protein levels. Thus, EW-7197 induced lipid accumulation.

HSCs are located between hepatocytes and sinusoidal endothelial cells in a quiescent state, and contribute to fibrosis by secreting ECM proteins or collagen in response to liver damage [23,24]. We attempted to reproduce TGF-β (2 ng/mL)-induced fibrosis in two types of hepatocytes: AML12 (mouse alpha hepatocytes) and LX-2 (human HSCs). EW-7197 inhibited TGF-β-induced increase in α-SMA, ColI, and p-SMAD2/3. Thus, EW-7197 effectively inhibited ECM accumulation, collagen deposition, and canonical pathway activation.

Fibrosis occurs during wound healing to prevent tissue decomposition in the presence of inflammation, apoptosis, and necrosis [25,26]. Early detection and treatment of liver fibrosis are important because symptoms appear only when the disease progresses from the mild to cirrhotic stage. Therefore, anti-fibrotic agents are urgently needed to prevent progression to the cirrhosis [27,28]. TGF-β is a potent inducer of fibrosis in various organs as it stimulates collagen I-rich ECM production in association with the progression of tissue fibrosis [7,9,29]. Thus, the ALK5 inhibitor EW-7197, a TGF-β signaling inhibitor, is a potentially effective drug that may prevent or eliminate the fibrosis-promoting effect.

Administering EW-7197 to cells and mice increased the number of lipid droplets, a previously unreported side effect. Fat accumulation increased when AML12 cells were treated with various concentrations of EW-7197 following TGF-β treatment, confirming this finding (Supplementary Fig. 4). Lipid droplet was observed in the liver even when the oral administration concentration was reduced to 5 mg/kg in an animal experiment (Supplementary Fig. 5). To identify the cause of the increase in lipid synthesis, we examined how EW-7197 affects non-canonical pathways. AMPK modulates several metabolic pathways, including hepatic lipid metabolism [30]. AMPK inhibits the transcription of adipogenic genes (carbohydrate response element binding protein [ChREBP]) by phosphorylating transcription factors such as Srebp1c [31,32]. Treating AML12 cells with TGF-β reduces AMPK, Erk, and Akt activation [33,34]. EW-7197 did not increase AMPK activity but significantly increased Erk and Akt activities. This suggests that EW-7197 can increase lipid synthesis by decreasing AMPK activity.

Combining TGF-β with Cur or Cur5-8 did not affect TGF-β-induced cell morphological changes or EMT as indicated by α-SMA staining. Similar analyses using AML12 and LX-2 cells showed that Cur5-8 reduced some fibrosis-related factors, although this effect was not significant, and the improvement was not as good as that observed using EW-7197. However, co-administering EW-7197 and Cur5-8 resulted in better improvement compared with administering each drug individually. Thus, co-administering EW-7197 and Cur5-8 decreased TGF-β-induced fibrosis in hepatocytes.

MCD is a classic diet-induced model of NASH that lacks methionine and choline, which are essential for mitochondrial β-oxidation and very-low-density lipoprotein synthesis in the liver [35]. The MCD diet thus causes hepatic steatosis. Furthermore, oxidative stress and changes in cytokines and adipose cytokines occur, contributing to liver damage and the accompanying fibrosis [36-38]. The body weights of 8-week-old C57BL/6 mice fed MCD for 6 weeks were significantly lower than Con group. A significant increase was observed in the weights of mice in the MCD+Cur5-8 and MCD+EW+Cur5-8 groups compared with mice in the MCD group. Levels of liver enzymes, including AST, ALT, and γ-GT, also significantly decreased in the MCD+EW+Cur5-8 group compared with the MCD group. Hydroxyproline levels also increased in the MCD+EW+Cur5-8 group. Similar results were also observed in the experiment in which EW-7197 was administered at 5 mg/kg (Supplementary Table 2, Supplementary Fig. 6).

Liver tissue biopsy is the standard procedure for estimating fibrosis. The NASH histological scoring system is called the NAS [39,40]. H&E staining was performed to determine the proportion of lipid droplets in hepatocytes, the degree of inflammation, and the extent of hepatocyte expansion, and the results were used to compute NAS. NASH was induced in the MCD group with a NAS score of 4.66±0.33, whereas administering both EW-7197 and Cur5-8 showed an improved NAS of 0.66±0.33. Sirius red and Masson's trichrome are the most common dyes used to estimate fibrosis and selectively bind to liver collagen, which causes fibrosis [41]. Sirius red and trichrome staining showed that fibrosis was induced in the MCD group compared with the Con group and that fibrosis was improved following co-administration of EW-7197 and Cur5-8. This suggests that co-administering EW-7197 and Cur5-8 effectively alleviates NASH-related conditions, including liver fibrosis.

Western blot analysis of homogenized liver tissue showed the degree of fibrosis based on protein levels. p-SMAD2/3, α-SMA, fibronectin, and ColI levels were higher in the MCD group than in the Con group, indicating an accumulation of the ECM.

This increase was significantly attenuated following co-administration of EW-7197 (20 mg/kg) and Cur5-8 (100 mg/kg).

Rock1 is an important regulator of energy balance and substrate metabolism, and tends to increase in metabolic disorders [42,43]. Srebp1c is a key transcription factor that regulates *de novo* lipogenesis in insulin-sensitive tissues, including liver, muscle, and adipose. Srebp1c activity is downregulated by the cellular energy sensor, AMPK [32,44,45]. Rock1 and Srebp1c levels were higher in MCD than in Con groups, but co-administering EW-7197 and Cur5-8 significantly decreased their levels. Furthermore, AMPK activity was lower in the MCD group than in the Con group but significantly increased when EW-7197 and Cur5-8 were co-administered (Fig. 2E and F). We expect that co-administering EW-7197 and Cur5-8 will effectively treat metabolic disorders.

ER stress describes a situation in which the amount of unfolded protein entering the ER exceeds the processing capacity of the organelle. This imbalance is recognized by inositol-requiring enzyme-1 (IRE1), ATF6, and PKR-like ER kinase (PERK) [46]. Nrf2 is a redox activator that controls the binding of the inhibitory protein Keap1, which is responsible for the cytoplasmic sequestration of Nrf2. Keap1 is a cysteine-rich protein that is anchored to the actin cytoskeleton and serves as an adapter protein for the Cul3-dependent E3 ubiquitin ligase complex. Under normal conditions, Keap1 promotes the ubiquitination and eventual degradation of Nrf2 [47]. The Keap1-Nrf2 pathway regulates the expression of numerous cytoprotective genes, including that encoding the antioxidant HO-1 [48]. The MCD diet induces unfolded protein response, increasing the expression of ATF6 associated with ER stress and decreasing the expression of components of the Nrf2-HO-1 pathway [49]. We showed that co-administering EW-7197 and Cur5-8 could improve ER stress and reduce ROS levels.

Although the MCD diet can induce hepatic steatosis or fibrosis in the short term, it is not appropriate compared with human NASH. In an animal model with symptoms similar to human NASH, we tried to induce NASH by providing an amylin diet (high-fat [40%], high cholesterol [2%]) and sugar water (42 g/L). Future experiments will check the beneficial effects of Cur5-8 and EW-7197 in this animal model. In this model, various indicators related to metabolism such as body weight, blood sugar, and insulin should be observed.

Beneficial effects were not observed for all parameters in the group in which Cur5-8 and EW-7197 were co-administered. However, EW-7197 significantly reduced fibrosis, and Cur5-8 inhibited the increase in lipid droplets in the liver by activating the AMPK pathway. Developing a drug that can improve fibrosis is important. This study shows that the Cur5-8 and EW-7197 combination can be used as a new treatment for NASH.

## SUPPLEMENTARY MATERIALS

Supplementary materials related to this article can be found online at https://doi.org/10.4093/dmj.2022.0110.

## CONFLICTS OF INTEREST

No potential conflict of interest relevant to this article was reported.

## AUTHOR CONTRIBUTIONS

Conception or design: K.B.H., E.S.L., N.W.P., S.H.J., S.S.
Acquisition, analysis, or interpretation of data: K.B.H.
Drafting the work or revising: K.B.H.
Final approval of the manuscript: D.K.K., C.M.A., C.H.C.

## ORCID

Kyung Bong Ha *https://orcid.org/0000-0002-6903-7253*
Choon Hee Chung *https://orcid.org/0000-0003-1144-7206*

## FUNDING

This work was supported by grant from the National Research Foundation of Korea (NRF) (2018R1A2B6005360, 2021R1A2B5B01002354). EW-7197 was generously provided by the Department of Pharmacy, College of Pharmacy, Ewha Womans University, and Seoul, Korea. The funders had no role in study design, data collection and analysis, decision to publish, or preparation of the manuscript.

## ACKNOWLEDGMENTS

None

## REFERENCES

1. Younossi ZM, Golabi P, de Avila L, Paik JM, Srishord M, Fukui N, et al. The global epidemiology of NAFLD and NASH in pa-

tients with type 2 diabetes: a systematic review and meta-analysis. J Hepatol 2019;71:793-801.
2. Younossi ZM, Koenig AB, Abdelatif D, Fazel Y, Henry L, Wymer M. Global epidemiology of nonalcoholic fatty liver disease-Meta-analytic assessment of prevalence, incidence, and outcomes. Hepatology 2016;64:73-84.
3. Chalasani N, Younossi Z, Lavine JE, Charlton M, Cusi K, Rinella M, et al. The diagnosis and management of nonalcoholic fatty liver disease: practice guidance from the American Association for the Study of Liver Diseases. Hepatology 2018;67:328-57.
4. Dufour JF, Caussy C, Loomba R. Combination therapy for non-alcoholic steatohepatitis: rationale, opportunities and challenges. Gut 2020;69:1877-84.
5. Iredale JP. Models of liver fibrosis: exploring the dynamic nature of inflammation and repair in a solid organ. J Clin Invest 2007;117:539-48.
6. Friedman SL. Mechanisms of hepatic fibrogenesis. Gastroenterology 2008;134:1655-69.
7. Leask A, Abraham DJ. TGF-beta signaling and the fibrotic response. FASEB J 2004;18:816-27.
8. Liu RM, Gaston Pravia KA. Oxidative stress and glutathione in TGF-beta-mediated fibrogenesis. Free Radic Biol Med 2010;48:1-15.
9. Friedman SL. Molecular regulation of hepatic fibrosis, an integrated cellular response to tissue injury. J Biol Chem 2000;275:2247-50.
10. Ooshima A, Park J, Kim SJ. Phosphorylation status at Smad3 linker region modulates transforming growth factor-β-induced epithelial-mesenchymal transition and cancer progression. Cancer Sci 2019;110:481-8.
11. Massague J, Wotton D. Transcriptional control by the TGF-beta/Smad signaling system. EMBO J 2000;19:1745-54.
12. Shi Y, Massague J. Mechanisms of TGF-beta signaling from cell membrane to the nucleus. Cell 2003;113:685-700.
13. Derynck R, Zhang YE. Smad-dependent and Smad-independent pathways in TGF-beta family signalling. Nature 2003;425:577-84.
14. Panahi Y, Hosseini MS, Khalili N, Naimi E, Simental-Mendia LE, Majeed M, et al. Effects of curcumin on serum cytokine concentrations in subjects with metabolic syndrome: a post-hoc analysis of a randomized controlled trial. Biomed Pharmacother 2016;82:578-82.
15. Kuptniratsaikul V, Dajpratham P, Taechaarpornkul W, Buntragulpoontawee M, Lukkanapichonchut P, Chootip C, et al. Efficacy and safety of Curcuma domestica extracts compared with ibuprofen in patients with knee osteoarthritis: a multicenter study. Clin Interv Aging 2014;9:451-8.
16. Jager R, Lowery RP, Calvanese AV, Joy JM, Purpura M, Wilson JM. Comparative absorption of curcumin formulations. Nutr J 2014;13:11.
17. Lee ES, Kwon MH, Kim HM, Woo HB, Ahn CM, Chung CH. Curcumin analog CUR5-8 ameliorates nonalcoholic fatty liver disease in mice with high-fat diet-induced obesity. Metabolism 2020;103:154015.
18. Jin CH, Krishnaiah M, Sreenu D, Subrahmanyam VB, Rao KS, Lee HJ, et al. Discovery of N-((4-([1,2,4]triazolo[1,5-a]pyridin-6-yl)-5-(6-methylpyridin-2-yl)-1H-imidazol-2-yl)methyl)-2-fluoroaniline (EW-7197): a highly potent, selective, and orally bioavailable inhibitor of TGF-β type I receptor kinase as cancer immunotherapeutic/antifibrotic agent. J Med Chem 2014;57:4213-38.
19. Park SA, Kim MJ, Park SY, Kim JS, Lee SJ, Woo HA, et al. EW-7197 inhibits hepatic, renal, and pulmonary fibrosis by blocking TGF-β/Smad and ROS signaling. Cell Mol Life Sci 2015;72:2023-39.
20. Kim MJ, Park SA, Kim CH, Park SY, Kim JS, Kim DK, et al. TGF-β type I receptor kinase inhibitor EW-7197 suppresses cholestatic liver fibrosis by inhibiting HIF1α-induced epithelial mesenchymal transition. Cell Physiol Biochem 2016;38:571-88.
21. Ha KB, Sangartit W, Jeong AR, Lee ES, Kim HM, Shim S, et al. EW-7197 attenuates the progression of diabetic nephropathy in db/db mice through suppression of fibrogenesis and inflammation. Endocrinol Metab (Seoul) 2022;37:96-111.
22. Rizki G, Arnaboldi L, Gabrielli B, Yan J, Lee GS, Ng RK, et al. Mice fed a lipogenic methionine-choline-deficient diet develop hypermetabolism coincident with hepatic suppression of SCD-1. J Lipid Res 2006;47:2280-90.
23. Josan S, Billingsley K, Orduna J, Park JM, Luong R, Yu L, et al. Assessing inflammatory liver injury in an acute CCl4 model using dynamic 3D metabolic imaging of hyperpolarized [1-(13)C]pyruvate. NMR Biomed 2015;28:1671-7.
24. Lepreux S, Desmouliere A. Human liver myofibroblasts during development and diseases with a focus on portal (myo)fibroblasts. Front Physiol 2015;6:173.
25. Issa R, Zhou X, Constandinou CM, Fallowfield J, Millward-Sadler H, Gaca MD, et al. Spontaneous recovery from micronodular cirrhosis: evidence for incomplete resolution associated with matrix cross-linking. Gastroenterology 2004;126:1795-808.

26. Popov Y, Sverdlov DY, Sharma AK, Bhaskar KR, Li S, Freitag TL, et al. Tissue transglutaminase does not affect fibrotic matrix stability or regression of liver fibrosis in mice. Gastroenterology 2011;140:1642-52.
27. Popov Y, Schuppan D. Targeting liver fibrosis: strategies for development and validation of antifibrotic therapies. Hepatology 2009;50:1294-306.
28. Friedman SL. Evolving challenges in hepatic fibrosis. Nat Rev Gastroenterol Hepatol 2010;7:425-36.
29. van Dijk F, Olinga P, Poelstra K, Beljaars L. Targeted therapies in liver fibrosis: combining the best parts of platelet-derived growth factor BB and interferon gamma. Front Med (Lausanne) 2015;2:72.
30. Viollet B, Lantier L, Devin-Leclerc J, Hebrard S, Amouyal C, Mounier R, et al. Targeting the AMPK pathway for the treatment of type 2 diabetes. Front Biosci (Landmark Ed) 2009;14:3380-400.
31. Kawaguchi T, Osatomi K, Yamashita H, Kabashima T, Uyeda K. Mechanism for fatty acid "sparing" effect on glucose-induced transcription: regulation of carbohydrate-responsive element-binding protein by AMP-activated protein kinase. J Biol Chem 2002;277:3829-35.
32. Li Y, Xu S, Mihaylova MM, Zheng B, Hou X, Jiang B, et al. AMPK phosphorylates and inhibits SREBP activity to attenuate hepatic steatosis and atherosclerosis in diet-induced insulin-resistant mice. Cell Metab 2011;13:376-88.
33. Hannon GJ, Beach D. p15INK4B is a potential effector of TGF-beta-induced cell cycle arrest. Nature 1994;371:257-61.
34. Datto MB, Li Y, Panus JF, Howe DJ, Xiong Y, Wang XF. Transforming growth factor beta induces the cyclin-dependent kinase inhibitor p21 through a p53-independent mechanism. Proc Natl Acad Sci U S A 1995;92:5545-9.
35. Anstee QM, Goldin RD. Mouse models in non-alcoholic fatty liver disease and steatohepatitis research. Int J Exp Pathol 2006;87:1-16.
36. Chowdhry S, Nazmy MH, Meakin PJ, Dinkova-Kostova AT, Walsh SV, Tsujita T, et al. Loss of Nrf2 markedly exacerbates nonalcoholic steatohepatitis. Free Radic Biol Med 2010;48:357-71.
37. Larter CZ, Yeh MM, Haigh WG, Williams J, Brown S, Bell-Anderson KS, et al. Hepatic free fatty acids accumulate in experimental steatohepatitis: role of adaptive pathways. J Hepatol 2008;48:638-47.
38. Leclercq IA, Farrell GC, Field J, Bell DR, Gonzalez FJ, Robertson GR. CYP2E1 and CYP4A as microsomal catalysts of lipid peroxides in murine nonalcoholic steatohepatitis. J Clin Invest 2000;105:1067-75.
39. Juluri R, Vuppalanchi R, Olson J, Unalp A, Van Natta ML, Cummings OW, et al. Generalizability of the nonalcoholic steatohepatitis Clinical Research Network histologic scoring system for nonalcoholic fatty liver disease. J Clin Gastroenterol 2011;45:55-8.
40. Kleiner DE, Brunt EM, Van Natta M, Behling C, Contos MJ, Cummings OW, et al. Design and validation of a histological scoring system for nonalcoholic fatty liver disease. Hepatology 2005;41:1313-21.
41. Asselah T, Marcellin P, Bedossa P. Improving performance of liver biopsy in fibrosis assessment. J Hepatol 2014;61:193-5.
42. Huang H, Lee SH, Sousa-Lima I, Kim SS, Hwang WM, Dagon Y, et al. Rho-kinase/AMPK axis regulates hepatic lipogenesis during overnutrition. J Clin Invest 2018;128:5335-50.
43. Gupta J, Gaikwad AB, Tikoo K. Hepatic expression profiling shows involvement of PKC epsilon, DGK eta, Tnfaip, and Rho kinase in type 2 diabetic nephropathy rats. J Cell Biochem 2010;111:944-54.
44. Ferre P, Foufelle F. SREBP-1c transcription factor and lipid homeostasis: clinical perspective. Horm Res 2007;68:72-82.
45. Wu W, Tang S, Shi J, Yin W, Cao S, Bu R, et al. Metformin attenuates palmitic acid-induced insulin resistance in L6 cells through the AMP-activated protein kinase/sterol regulatory element-binding protein-1c pathway. Int J Mol Med 2015;35:1734-40.
46. Ron D, Walter P. Signal integration in the endoplasmic reticulum unfolded protein response. Nat Rev Mol Cell Biol 2007;8:519-29.
47. Kobayashi M, Yamamoto M. Nrf2-Keap1 regulation of cellular defense mechanisms against electrophiles and reactive oxygen species. Adv Enzyme Regul 2006;46:113-40.
48. Alam J, Stewart D, Touchard C, Boinapally S, Choi AM, Cook JL. Nrf2, a Cap'n'Collar transcription factor, regulates induction of the heme oxygenase-1 gene. J Biol Chem 1999;274:26071-8.
49. Yen IC, Tu QW, Chang TC, Lin PH, Li YF, Lee SY. 4-Acetylantroquinonol B ameliorates nonalcoholic steatohepatitis by suppression of ER stress and NLRP3 inflammasome activation. Biomed Pharmacother 2021;138:111504.